

Disorder and the effective Mn-Mn exchange interaction in $\text{Ga}_{1-x}\text{Mn}_x\text{As}$ diluted magnetic semiconductors

Antônio J. R. da Silva,¹ A. Fazzio,¹ Raimundo R. dos Santos,² and Luiz E. Oliveira³

¹*Instituto de Física, Universidade de São Paulo, CP 66318, 05315-970, São Paulo SP, Brazil*

²*Instituto de Física, Universidade Federal do Rio de Janeiro, CP 68528, 21945-970 Rio de Janeiro RJ, Brazil*

³*Instituto de Física, Unicamp, CP 6165, 13083-970 Campinas SP, Brazil*

(Dated: Version 1.9 – 8th February 2020)

We perform a theoretical study, using *ab initio* total energy density-functional calculations, of the effects of disorder on the $\text{Mn} - \text{Mn}$ exchange interactions for $\text{Ga}_{1-x}\text{Mn}_x\text{As}$ diluted magnetic semiconductors. For a 128 atoms supercell, we consider a variety of configurations with 2, 3 and 4 Mn atoms, which correspond to concentrations of 3.1%, 4.7%, and 6.3%, respectively. In this way, the disorder is intrinsically considered in the calculations. Using a Heisenberg Hamiltonian to map the magnetic excitations, and *ab initio* total energy calculations, we obtain the effective $J_n^{\text{Mn-Mn}}$, from first ($n = 1$) all the way up to sixth ($n = 6$) neighbors. Calculated results show a clear dependence in the magnitudes of the $J_n^{\text{Mn-Mn}}$ with the Mn concentration x . Also, configurational disorder and/or clustering effects lead to large dispersions in the Mn-Mn exchange interactions, in the case of fixed Mn concentration. Moreover, theoretical results for the ground-state total energies for several configurations indicate the importance of a proper consideration of disorder in treating temperature and annealing effects.

PACS numbers: 71.55.Eq, 75.30.Hx, 75.50.Pp

I. INTRODUCTION

The exciting possibilities of manipulating both the spin and the charge of the carriers in semiconductors, in such a way that new devices may be designed, have brought a lot of attention to the study of diluted magnetic semiconductors (DMS) in the past ten years or so. Even though the DMS have been known for a long time,¹ it was the discovery of ferromagnetism in p-type (In,Mn)As systems² that spurred the research in this field. This was even more so after the successful growth of ferromagnetic (Ga,Mn)As alloys.³ This latter system has become almost a paradigm in the field of DMS materials. It has long been known that isolated Mn_{Ga} substitutional impurities give rise to acceptor states around 0.1 eV above the top of the valence band. Thus, the Mn atoms have a double functionality in the $\text{Ga}_{1-x}\text{Mn}_x\text{As}$ alloys: they provide both (i) the magnetic moments, and (ii) holes to intermediate the interaction between them. This somewhat simplistic view is much more complex than it seems at first sight. Ferromagnetism in $\text{Ga}_{1-x}\text{Mn}_x\text{As}$ only occurs for large Mn concentrations of a few percent. As a consequence, the acceptor levels form a band which, due to the rather localized character of the defect state, has a dispersion which is far from what would result from a free quasi-particle picture. Moreover, the intrinsic disorder coupled to this somewhat narrow band indicates that any theoretical description based on an effective mass description should be viewed with caution. To further complicate the issue, in order to obtain the necessary high Mn concentrations the growth temperatures cannot be too high, which causes a lot of defects to be present in the samples, like Mn interstitials (Mn_I) and arsenic antisites (As_{Ga}). As a result, the critical temperature and hole concentration, as

a function of Mn composition, are crucially dependent on the details of growth conditions.^{4,5,6,7,8,9,10,11,12,13,14,15,16}

In view of all these facts, it would be important to have a way to estimate the Mn-Mn exchange interactions (i) with as few assumptions as possible, (ii) which would treat the host and the Mn impurities at the same level of accuracy, and (iii) which would furthermore include the effects of disorder. This approach of implicitly tracing out the holes degrees of freedom has been implemented in a variety of ways based on self-consistent methods. Van Schilfgaarde and Mryasov¹⁷ have performed calculations of total energies, within the atomic spheres approximation, to extract exchange couplings, J 's, for specific (*i.e.*, not randomly chosen) clusters of closely spaced Mn ions; their results suggest a tendency of a decrease in $|J|$ when more Mn atoms are added to nearby sites. More recently, Xu *et al.*¹⁸ used muffin-tin orbitals to investigate the dependence of the exchange coupling with the Mn-Mn distance at much larger (8.3%) concentrations of Mn atoms; they found a considerable scatter in the values of the exchange couplings. In a series of theoretical studies, in which the effect of randomness/disorder is described by the coherent-potential approximation (CPA), Kudrnovský *et al.*^{19,20} and Bergqvist *et al.*²¹ have used a tight-binding linear muffin-tin orbital method, together with the magnetic force theorem, to study the dependence of the Mn-Mn exchange couplings and critical temperatures with the concentration of Mn impurities in III-V and group IV DMS. Also, Sato *et al.*^{22,23} have used muffin-tin type potentials together with a KKR-CPA approach to study Curie temperatures and exchange interactions in III-V DMS. Moreover, Sandratskii and Bruno^{24,25,26} have used the augmented-spherical-wave method within the local-density approxi-

mation to investigate exchange interactions, Curie temperatures and the influence of the clustering of Mn impurities in (Ga,Mn)As. One should notice that the use of non-full potential muffin-tin-style approaches is not adequate to treat the electronic structure of covalent semiconductor systems such as (Ga,Mn)As DMS. Furthermore, we will show that disorder plays an important role which may not be adequately treated by simple effective-medium approaches such as the virtual crystal approximation (VCA) or CPA.

In this work we perform large supercell total energy calculations, based on *ab initio* density functional theory (DFT) methods. Within this approach, we treat disorder configurations in which the Mn atoms randomly replace Ga atoms. By considering two, three, and four Mn atoms in a supercell with 128 atoms, we cover three Mn concentrations, 3.1%, 4.7%, and 6.3%, and present results for the effective exchange interactions, $J_n^{\text{Mn-Mn}}$, between two Mn atoms which are n -th neighbors in the Ga sublattice, with $1 \leq n \leq 6$. Also, in a few cases the Mn atoms are placed in predetermined positions, in order to compare the exchange coupling of two nearest-neighbor Mn atoms in the presence of other Mn atoms, placed at various separations. The present results indicate a clear decrease in the magnitudes of the $J_n^{\text{Mn-Mn}}$ with the Mn concentration x ; from now on, the Mn-Mn superscript in $J_n^{\text{Mn-Mn}}$ will be omitted, in order to simplify the notation.

The work is organized as follows. In Section II we provide a brief description of the calculational procedure used in the present study. Results and discussion are left for Section III, and Section IV summarizes our findings and conclusions.

II. CALCULATIONAL METHOD

We have performed total energy calculations based on the density-functional theory (DFT) within the generalized-gradient approximation (GGA) for the exchange-correlation potential, with the electron-ion interactions described using ultrasoft pseudopotentials.²⁷ A plane wave expansion up to 230 eV as implemented in the VASP code²⁸ was used, together with a 128-atom fcc supercell and 4 L -points for the Brillouin zone sampling; these L -points are non-equivalent, due to the presence of Mn impurities. The positions of all host GaAs atoms as well as substitutional Mn in the supercell were relaxed until all the forces components were smaller than 0.02 eV/Å; our GGA lattice parameter for undoped GaAs turned out to be 5.74 Å, which is in accordance with other estimates, e.g., that of Ref. 29. For a 128 atoms supercell, we consider a variety of configurations with 2, 3 and 4 Mn atoms, corresponding to concentrations of 3.1%, 4.7%, and 6.3%, respectively. Since calculations for *all* possible disorder configurations with more than 2 Mn atoms per cell is prohibitively costly in terms of computer time, we have considered *typical* configurations, as gener-

ated through the Special Quasi-random Structures (SQS) algorithm.³⁰ A configuration σ is generated by placing the Mn atoms at Ga sublattice sites (64 possible sites). We then calculate the pair correlation functions, up to the sixth-neighbor, given by:

$$\Pi_m(\sigma) = \frac{1}{64Z_m} \sum_{i,j} \Delta_m(i,j) S_i S_j. \quad (1)$$

Here Π_m is the m th-neighbor pair correlation function, Z_m is the number of m th-order neighbors to a site, $\Delta_m(i,j)$ is 1 if sites i and j are m th-order neighbors, and zero otherwise; and S_i is a variable taking values 0, if site i is occupied by Ga, and 1 if it is occupied by Mn. For a perfectly random (R) distribution of Mn atoms, the pair correlation function does not depend on m , $\Pi_m(R) = x^2$, where x is the Mn concentration. For a given configuration we calculate the deviation from randomness as

$$\delta\Pi(\sigma) = \sum_m (\Pi_m(\sigma) - \Pi_m(R))^2. \quad (2)$$

The above quantity indicates how random the σ configuration is. We perform an exhaustive search over all possible configurations and choose to work with the ones with lowest $\delta\Pi$.

For each chosen disorder configuration, we adopt the following strategy within our DFT-GGA calculations. As an initial guess, we take all valence electrons of each Mn atom aligned with each other, corresponding to $S = 5/2$ as expected in a d^5 configuration, and calculate the total energies for this configuration, as well as for an increasing number of flipped Mn total spins. The energy differences with respect to the aligned states, $\{\Delta E\}$, are then described by an effective Heisenberg model with appropriate first-, second-, and so forth, up to sixth-nearest-neighbor Mn-Mn couplings, J_n , $n = 1 - 6$; see Sec. III and Appendix for details. This procedure has been applied^{31,32} to the case of two Mn atoms in a supercell with 128 sites, and we were able to infer the dependence of the effective couplings with both the Mn-Mn distance and direction. We have found^{31,32} that the calculated J_n exchange couplings lead to a Mn ferromagnetic state, with the holes forming a relatively dispersionless impurity band, and therefore that a conventional free-electron-like RKKY interaction should be ruled out as the origin of the Mn-Mn ferromagnetic coupling.

One should notice that for two Mn atoms, if the spins are treated quantum mechanically the above mentioned energy difference corresponds to that between the state with total spin 5/2 and the singlet one, leading to $J_n^{(Q)} = \Delta E_n/15$. If the spins are treated classically, $J_n^{(Cl)} = 2\Delta E_n/25$ and the two approaches are entirely equivalent, apart from an overall multiplicative factor of 1.2. For more than two Mn atoms, we consider classical spins and note that this approximation, though not capturing full details of the excitation spectra, is still able

to provide overall trends of the low energy magnetic excitations for a finite number of spins.

As a final methodological comment, we note that we have checked for spin-orbit effects (in the case of two Mn atoms) through the projector augmented-wave (PAW) method³³, and found a change from 0.29 eV to 0.24 eV in the total energy difference between the excited anti-ferromagnetic and ground state ferromagnetic Mn-spin alignments. Although a systematic study in this sense would certainly be important, this is beyond the scope of the present study and we have chosen to ignore spin-orbit effects in the total energy calculations presented in this work. We believe this approximation would not alter the general conclusions of the present study. Moreover, other possibilities, such as a non-collinear ferromagnetism,^{34,35} have not been considered at this stage.

III. RESULTS AND DISCUSSION

A. Two Mn atoms

Let us first discuss the case of two Mn substitutional atoms in the 128-site supercell. We considered *all* configurations corresponding to all inequivalent positions within the supercell, i.e., Mn-Mn distances varying from 4.06 Å up to 11.48 Å. Our total energy results yield a Mn-Mn ferromagnetic ground state in all cases. The relevant Heisenberg Hamiltonian in this case is

$$H = J_n \mathbf{S}_i \cdot \mathbf{S}_{i+\mathbf{n}}, \quad (3)$$

for each relative position in the supercell, where, for the sake of comparison with the cases of three and four Mn atoms (see below), \mathbf{S} is taken as a classical spin of magnitude 5/2; \mathbf{n} is a vector connecting n th-nearest-neighbor Mn atoms replacing Ga atoms. The estimates for J_n thus obtained are displayed in the second column of Table I.

As previously noted,^{31,32} the resulting Mn-Mn ferromagnetic effective coupling in $\text{Ga}_{1-x}\text{Mn}_x\text{As}$ is essentially intermediated by the antiferromagnetic coupling of each Mn spin to the quasi-localized holes. Also, the observed non-monotonic behavior of J_n should be attributed to the anisotropic character of the effective interaction. Moreover, $|J_n|$ essentially decreases^{31,32} with Mn-Mn separation and vanishes above ~ 11.5 Å.

B. Three Mn atoms

In the case of three Mn atoms in a supercell with 128 sites, we have performed calculations for 10 different disorder configurations. Figure 1 shows two SQS illustrative configurations: in (a) the 3 Mn atoms are somewhat clustered together, whereas in (b) two are nearest neighbors and the third is farther apart.

For each disorder configuration, the relevant Heisenberg Hamiltonian must contemplate the possibility of interactions occurring not only amongst spins within the

Table I: Estimates for the effective exchange coupling, J_n , in meV, between n th-nearest-neighbor Mn spins, \mathbf{S}_i and \mathbf{S}_j , for different Mn concentrations, x . In the case of 2 Mn atoms ($x = 3.1\%$), J_n is unique for a given n . For 3 Mn atoms ($x = 4.7\%$) in a supercell with 128 sites, we have performed calculations for 10 different SQS disorder configurations, and J_n is given by the average over the configurations in which two Mn sites are n th-neighbors; the number of such configurations are shown in square brackets, and the error bars are calculated as standard deviation of averages. In the case of 4 Mn atoms ($x = 6.3\%$), we show the results for two configurations (see text); note that sometimes a specific configuration would not accommodate the pertinent J_n .

n	$x = 3.1\%$	$x = 4.7\%$	$x = 6.3\%$	$x = 6.3\%$
1	-23.2	-18.2 ± 1.5 [7]	-12.6	-13.0
2	-10.4	-3.8 ± 1.8 [4]	-	-4.7
3	-13.6	-6.6 ± 2.7 [7]	-2.8	-6.0
4	-5.6	-3.6 ± 0.8 [4]	-4.8	-
5	-2.6	$+0.4 \pm 0.7$ [5]	+0.1	-1.3
6	-4.4	-1.9 ± 0.7 [2]	-	-

supercell, but between one spin in the supercell and the different images in neighboring supercells (periodic boundary conditions effects, PBCE's). In actual fact, depending on the disorder configuration, the same pair of spins may be j -th nearest neighbors within the supercell and k -th nearest neighbors when the images are considered. One can therefore write the Hamiltonian as

$$H = \sum_n \sum_{i < j} w_{ij}(n) J_n \mathbf{S}_i \cdot \mathbf{S}_j, \quad (4)$$

where the $w_{ij}(n)$ are geometrical weights taking into account PBCE's. For a given configuration, one expects most of the w 's to vanish; also, we set $w = 0$ if the distance between the Mn atoms is larger than 11.5 Å, as previously established.³² In the Appendix we discuss the Hamiltonian for the two SQS configurations of Fig. 1. We then calculate the total energies for different Mn spin configurations: with all spins aligned, with only one spin reversed, either in site 1, 2, or 3, and so forth, increasing the number of spin flips, until one has the same number of unknowns (J_n) as equations (namely, the corresponding energy differences with respect to the aligned state).

It is instructive to lay out J_n as a function of n for the 10 SQS realizations of disorder (three Mn atoms), as shown in Fig. 2; for comparison, we show the results for $x = 3.1\%$ in the same figure. One can see that the overall trend of J_n with n , observed in the case of two Mn spins, is maintained in this case, with the non-monotonic behavior still being due to effects of directionality, i.e., the exchange coupling depends not only on the distance between the pair of Mn atoms, but also on their relative direction with respect to the bonds of the host GaAs. Here we should mention that our 128-atom supercell total energy results for the ferro- and antiferromagnetic

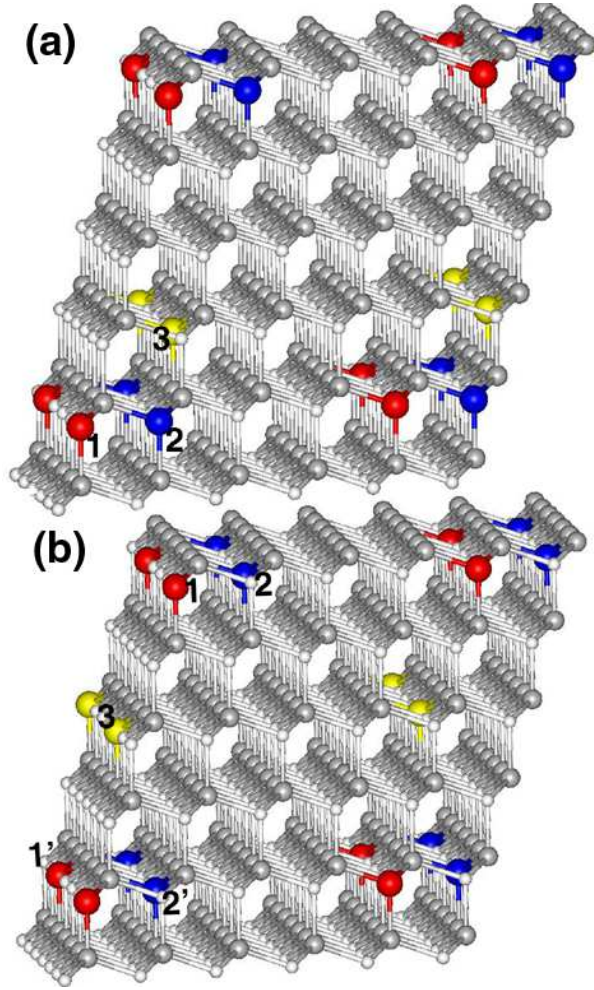


Figure 1: (Color online) A pictorial view of two possible realizations of disorder for three Mn atoms in a 128-site supercell ($x = 4.7\%$). Ga sites are represented by the smaller spheres, As sites by the middle-sized ones, and Mn atoms by the largest ones. For clarity, supercells are repeated along the different cartesian directions. The three nonequivalent Mn atoms are shown as different shades of gray (blue, red, and yellow in the color version).

states are in overall agreement with the corresponding 64-atom supercell total energy results of Mahadevan *et al.*³⁶ The corresponding average values of J_n , for each n , are shown in the third column of Table I. It is interesting to note that all J_n decrease (in absolute value) as the concentration of Mn atoms increases from 3.1% to 4.7%. While at first sight this may seem an unusual behavior, one should have in mind that the effective Mn-Mn interaction is hole-mediated, thus sensitive to the hole density.

In order to assess the effects of clustering in a systematic way, we have also considered non-SQS configurations in which two Mn atoms are first neighbors, and a third Mn atom is placed in positions corresponding to fifth-, third-, and first-neighbor of the pair: we found that $J_1 = -20.8$ meV, -17.3 meV, and -8.1 meV, respectively; the extreme values are shown in Fig. 2 as filled

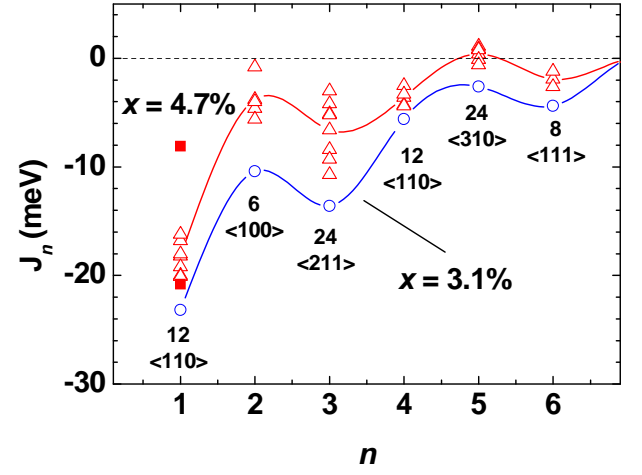


Figure 2: (Color online) The n th-nearest-neighbor exchange coupling as a function of n for $x = 3.1\%$ and $x = 4.7\%$ (with data displayed for 10 SQS configurations, see text). Full curves are guides to the eye (for $x = 4.7\%$ the full line goes through average values of J_n). Filled squares for J_1 correspond to extreme values obtained for the non-SQS configurations; see text. Also shown is the multiplicity of each n -th neighbor pair in a given direction $\langle hkl \rangle$.

Table II: Total energies from ferromagnetic SQS configurations, labelled from $\ell = 1$ to 10, with respect to the total energy of the configuration corresponding to three nearest-neighbor Mn atoms clustered together. The effective Heisenberg Hamiltonian can be written in the form $H = \alpha J_i \mathbf{S}_1 \cdot \mathbf{S}_2 + \beta J_j \mathbf{S}_1 \cdot \mathbf{S}_3 + \gamma J_k \mathbf{S}_2 \cdot \mathbf{S}_3$, such that the entries in the third column are $\{i^\alpha j^\beta k^\gamma\}$

ℓ -th state	E_ℓ (eV)	$\{i^\alpha j^\beta k^\gamma\}$
1	0.054	$\{1^1 3^1 4^2\}$
2	0.077	$\{1^1 4^2 5^2\}$
3	0.085	$\{1^1 3^1 3^1\}$
4	0.090	$\{1^1 3^1 6^4\}$
5	0.091	$\{1^1 3^1 5^2\}$
6	0.103	$\{1^1 2^1 3^1\}$
7	0.125	$\{1^1 2^1 5^2\}$
8	0.158	$\{2^1 4^2 6^4\}$
9	0.176	$\{3^1 4^2 5^2\}$
10	0.227	$\{2^1 3^1 5^2\}$

squares. Thus, *clustering tends to weaken the magnitude of the nearest-neighbor coupling*. One may attribute this behavior as most likely resulting from the Coulomb repulsion between the holes, which leads to their delocalization as the Mn atoms group together, being therefore detrimental of their role as mediators of ferromagnetism.

If, on the one hand, clustering tends to decrease the magnitude of the nearest-neighbor exchange, on the other hand it leads to the energetically most stable configuration; this is in agreement with recent results from calculations restricted to pairs of transition metals.³⁷ In Table II we display the energies of calculated ferromagnetic

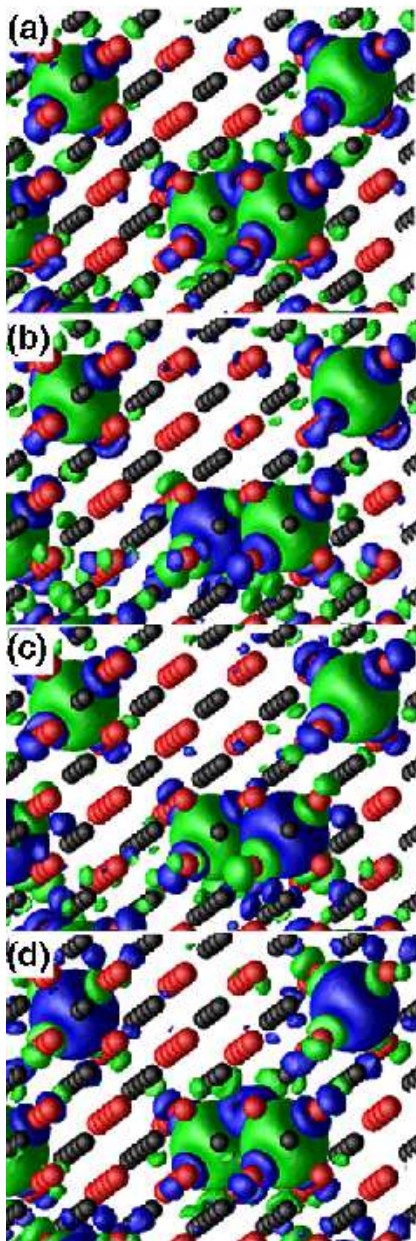


Figure 3: (Color online) Isosurfaces for the net local magnetization $m(\mathbf{r})$ (see text for definition) in the case of three Mn_{Ga} defects [for the configurations depicted in Fig. 1(a)], with (a) all spins aligned and (b)-(d) only one flipped spin. The green surface corresponds to a value of $+0.005 e/\text{\AA}^3$, and the blue surface to $-0.005 e/\text{\AA}^3$, with e being the electron charge. The black (red) spheres denote the Ga (As) atoms.

SQS configurations relative to the clustered one in which the three Mn atoms are first-nearest neighbors. We note that the SQS configurations labelled from 8 to 10, which have the highest total energies of the set, correspond to cases in which there are no first-neighbor pairs of Mn atoms. Since $\text{Ga}_{0.97}\text{Mn}_{0.03}\text{As}$ is only stable at growth temperatures in the range 200–300 C,^{6,38} the scale of energies shown in Table II indicates that not many config-

urations can be thermally activated. Clearly, there are several other mechanisms at play – such as mobility of Mn atoms, possibility of trapping on interstitials, and so forth –, which are not included in the present approach, and will determine the final distribution of Mn atoms.

Figures 3(a)-(d) show the net magnetization $m(\mathbf{r}) \equiv \rho_{\uparrow}(\mathbf{r}) - \rho_{\downarrow}(\mathbf{r})$, where ρ_{σ} is the total charge density in the σ -polarized channel, for three Mn atoms with all spins aligned and for only one flipped spin, for the configuration depicted in Fig. 1 (a). Note that the densities on the upper right and upper left corners in each figure are related to a Mn atom and its image in a neighboring supercell. Similarly to the $m(\mathbf{r})$ of one³¹ and two Mn impurities³² in a supercell, near each Mn atom the local magnetization has a d_{σ} -like character, whereas close to the As neighbors, the character changes to $p_{\bar{\sigma}}$ -like, where $\sigma = (\uparrow \text{ or } \downarrow)$ and $\bar{\sigma} = (\downarrow \text{ or } \uparrow)$. Also, $m(\mathbf{r})$ has a rather localized character. The flipping of spins introduce nodes on the $m(\mathbf{r})$ and subtle changes mostly on the orientation of the p -like lobes. Close to the Mn atoms, however, the local magnetization is not very sensitive to the flips.

C. Four Mn atoms

For four Mn atoms, we have considered only two disorder configurations, chosen according to the SQS algorithm. A Hamiltonian similar to Eq. (4) may be written, with the addition of terms involving the fourth spin, having in mind that the interactions with spins on image sites are more frequent in this case.

For instance, in one of the calculated SQS configurations, the effective Hamiltonian becomes

$$H = 2J_5\mathbf{S}_1 \cdot \mathbf{S}_2 + J_1\mathbf{S}_1 \cdot \mathbf{S}_3 + J_3\mathbf{S}_1 \cdot \mathbf{S}_4 + 2J_4\mathbf{S}_2 \cdot \mathbf{S}_3 + J_3\mathbf{S}_2 \cdot \mathbf{S}_4 + J_1\mathbf{S}_3 \cdot \mathbf{S}_4, \quad (5)$$

where the absence of a J_2 second-neighbor interaction should be noticed. Calculations of total energies for all Mn spins parallel, and for the four possible single flips, lead to four excitation energies, from which the J_n 's ($n \neq 2$) may be inferred. Analogous considerations apply to the other SQS configuration. The results are shown in columns 4 and 5 of Table I. One sees that the overall tendency of J_n is to decrease in magnitude as n is increased, in a pattern similar to that for smaller concentrations, though the dispersion cannot be properly assessed due to the scarcity of data. We also note that, as in the case of three Mn atoms, calculations with a non-SQS configuration with the four Mn atoms clustered together indicate that clustering decreases the magnitude of the first-neighbor J_1 exchange coupling: $J_1 = -6.5$ meV in this case, which should be compared with the -12.6 meV and -13.0 meV values of Table I.

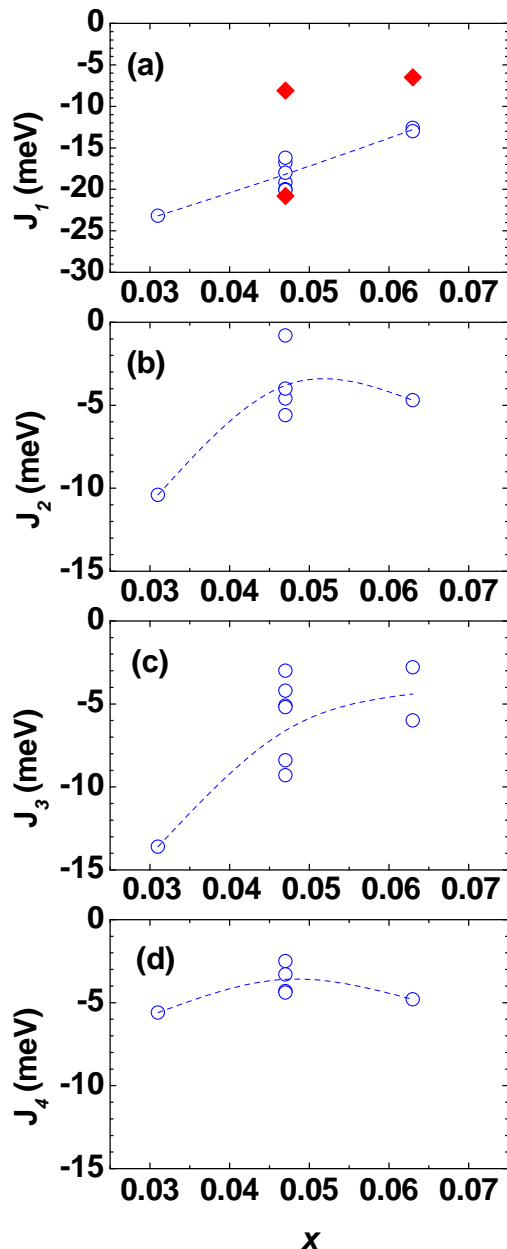


Figure 4: (Color online) Dependence of: (a) J_1 , (b) J_2 , (c) J_3 , and (d) J_4 with the concentration of Mn atoms. For $x = 3.1\%$, J_n is unique for a given n . Values for the SQS configurations are shown as empty circles, while the filled diamonds correspond to the extreme values obtained for the non-SQS configurations; see text. Dotted curves are guides to the eye through the average values of J_n .

D. The dependence of J_n with the concentration

The data in Table I can also be used to discuss the dependence of J_n with x , for a given n . In Fig. 4 we plot J_1 , J_2 , J_3 and J_4 as functions of x . For the case of J_1 , we also show (as filled symbols) three values obtained for the non-SQS configurations: two as mentioned before, in the case of three Mn atoms, and the one cor-

responding to four Mn atoms clustered together as first nearest-neighbors.

From Fig. 4, we see that, in most cases, the magnitudes of the exchange couplings decrease as the concentration of Mn atoms is increased. Further, this decrease may be quite significant; for instance, the magnitude of the average J_1 decreases by the order of 50% when one roughly doubles the concentration from 3.1%. We also see that for the configurations in which the Mn atoms are clustered together, $|J_1|$ also decreases as x is increased. This overall decrease with x can be taken as numerical evidence that a steady increase in the concentration of Mn atoms is not sufficient to rise the critical temperature, since the exchange couplings will eventually be weakened. Clearly other effects may be playing important roles. For instance, within our present approach, the hole density is assumed to be the same as that of Mn atoms, which, as mentioned in the Introduction is not really the case. The presence of Mn interstitials and Mn-As complexes also need to be taken into account in order to reach a quantitative agreement. Nonetheless, one expects that the trends unveiled here are indicative of the actual experimental situation.

It is important to have in mind that several theoretical works have previously examined the dependence of the exchange couplings with the Mn-Mn separation or with the Mn concentration.^{18,19,20,21,22,23,24,25,26} Some predict an alternating sign for the exchange coupling, but these predictions should be taken with extreme care, since these theoretical calculations are based on non-full-potential muffin-tin-type potentials which are not reliable to treat the electronic structure of covalent semiconductor systems such as (Ga,Mn)As DMS. Also, disorder quite certainly is not adequately taken into account within simple effective-medium approaches such as VCA or CPA, as fluctuations in the Mn positions essentially lead to variations in the Mn-Mn exchange-coupling parameters, as apparent from Fig. 4.

IV. CONCLUSIONS

We have performed *ab initio* total energy density-functional calculations for two, three, and four substitutional Mn atoms in a 128 atoms supercell, corresponding to concentrations of 3.1%, 4.7%, and 6.3%, respectively. In this way, we have treated the host and the Mn impurities on equal footing. The effects of disorder have been assessed at different levels of approximations, depending on the concentration of Mn atoms: for $x = 3.1\%$, *all* possible non-equivalent positions of the Mn atoms have been considered; for $x = 4.7\%$, ten non-equivalent configurations have been generated through the SQS algorithm, while three specific ones have also been considered in order to discuss the effects of clustering; and, for $x = 6.3\%$, two SQS and one non-SQS configurations have been investigated. While the relation between the densities of holes and of Mn atoms is

one of the yet unsolved issues in the context of DMS, here we have assumed that each Mn atom provides one hole; since our results relate to general trends, they may be carried over to the actual experimental situation of only a fraction of Mn atoms contributing with holes. It is also interesting to note that the cut-off of 11.5 Å (which would correspond to $x \simeq 0.042$) imposed on the range of Mn-Mn exchange couplings would appear to be in direct contradiction with experimental data by Edmonds et al.⁸, according to which ferromagnetism is seen for dopings as low as ~ 0.015 (where one would have essentially no compensation). Since the site percolation threshold⁴⁰ for FCC lattices is 0.20, for the Ga FCC sublattice in (Ga,Mn)As, the concentration cut-off for ferromagnetic order would be of the order of $0.20 \times 0.042 = 0.0084$, i.e., $x \simeq 0.84\%$, indicating that there is no contradiction with the measurements of Edmonds et al.⁸

We have focused mainly on the effective exchange interaction between Mn spins, by mapping the spectra of magnetic excitations (spin flips) onto a classical Heisenberg Hamiltonian with coupling constants J_n , ranging from first ($n = 1$) to sixth ($n = 6$) nearest neighbors. The effects of clustering on the nearest-neighbor pair-exchange coupling, J_1 , have been investigated by examining specific (i.e., non-random) configurations with three and four Mn atoms in the 128-site supercell: We have established that clustering tends to weaken the magnitude of the nearest-neighbor exchange coupling. On the other hand, we have found that clustered structures of Mn atoms have the lowest total energies, a result which may be of importance in a realistic discussion of annealing and/or diffusion effects. From calculations on random configurations we have also been able to determine the behavior of J_n with x , for fixed n : in most cases the exchange couplings get weaker as the concentration of Mn atoms is increased. This is consistent with the experimentally observed fact that there is an optimum range of Mn concentrations (whose quantitative determination requires a careful consideration of other disorder effects) in which the critical temperatures are the highest.

For fixed Mn density, we have found that the calculated J_n favor a ferromagnetic ground state, and have decreasing magnitude as the distance between spins increases (cf. Table I and Figs. 2 and 4). The non-monotonic behavior is attributed to directionality effects; by the same token, deviations in the sign of J_n were found only at large n ($=5$), when its magnitude is already greatly reduced with respect to the nearest neighbor value. The discrepancy of the present results with respect to recent calculations by Xu *et al.*,¹⁸ may be attributed to the fact that their muffin-tin calculations are not full potential; they therefore do not fully reproduce the crucial role played by the directional sp^3 bonds and by the hole p -states. Also, due to the quite significant variations of the calculated exchange couplings with configurations and Mn concentration, we emphasize that estimates of the critical temperature obtained via exchange couplings thus obtained are clearly open to

question. We should also stress that the present results corroborate that the Mn-Mn ferromagnetic effective coupling in $\text{Ga}_{1-x}\text{Mn}_x\text{As}$ is intermediated by *localized* holes leading to an antiferromagnetic (non-RKKY) coupling of each Mn spin, as previously noted,^{31,32} and recently confirmed experimentally.³⁹ Therefore, the inescapable conclusion is that the main feature of a conventional free-electron-like or perturbative RKKY interaction should be ruled out^{41,42} in the case of $\text{Ga}_{1-x}\text{Mn}_x\text{As}$.

As a final point, some comments regarding future perspectives are in order. From one side, investigations using a similar procedure as employed here (where the disorder is explicitly included) of how impurities, such as interstitial Mn and As anti-sites, alter the effective exchange interactions are relevant. For a given Mn configuration, it should be interesting to see how the results depend on the relative position of the defects. On the other hand, our results raise some questions whose answers are not completely trivial: (i) The fact that the effective exchange interactions change with the Mn configuration make it clear that the use of a Heisenberg model, at least a simple one where only pair-interactions are considered, should be viewed with caution. It is not obvious that extensions of the Heisenberg model to triplets or even larger cluster interactions will remedy this fact; (ii) The use of *ab initio* calculations has been very important in order to provide a correct picture of the electronic structure of these systems. One of its great merits is the possibility of obtaining model-free results. However, whenever one needs to make predictions about the critical temperature (T_c), models have to be used. For instance, from *ab initio* results one may extract effective exchange parameters, as in the present work, and then via mean field or more sophisticated methods, like Monte Carlo calculations, it is possible to calculate T_c . Two crucial steps in this procedure are questionable. The first one is the use of a Heisenberg model, as already mentioned. The other is the use of a small supercell approximation. Calculating the critical temperature via any effective methodology that is based on *small* supercell *ab initio* calculations, even if this effective approach allows the search of a large number of distinct configurations, has a great risk of being nonsense, since, as we have shown, the exchange interactions depend sensitively on the Mn distribution. The root of the above problems is the necessity of introducing a model hamiltonian in order to extract excited states of the system associated with spin excitations. A possible solution to this problem could be the use of a semi-empirical hamiltonian with a tight-binding description for the host material coupled with a many-body, atomic-like description for the Mn atoms. The manifold of low-energy states representing the different Mn spin orientations, that will be obtained upon diagonalization of such a hamiltonian⁴³, will replace the states obtained via the effective (but questionable) Heisenberg hamiltonian.

Acknowledgments

Partial financial support by the Brazilian Agencies CNPq, CENAPAD-Campinas, Rede Nacional de Materiais Nanoestruturados/CNPq, FAPESP, FAPERJ, and Millenium Institute for Nanosciences/MCT is gratefully acknowledged.

Appendix

Here we discuss the case of three Mn atoms, for the two disorder configurations displayed in Figs. 1(a) and 1(b), and chosen according to the SQS algorithm. For the configuration in Fig. 1(a) ($\ell = 4$ in Table II), the Hamiltonian [see Eq. (4)] may be written, having in mind that the interactions with spins on image sites are to be taken into account, as

$$H = J_1 \mathbf{S}_1 \cdot \mathbf{S}_2 + J_3 \mathbf{S}_2 \cdot \mathbf{S}_3 + 4J_6 \mathbf{S}_1 \cdot \mathbf{S}_3 \quad (\text{A.1})$$

where the absence of second-neighbor, fourth-neighbor, and fifth-neighbor interactions should be noticed.

In a similar way, for the configuration in Fig. 1(b) ($\ell = 9$ in Table II), the Hamiltonian is given by

$$H = J_3 \mathbf{S}_1 \cdot \mathbf{S}_2 + 2J_4 \mathbf{S}_1 \cdot \mathbf{S}_3 + 2J_5 \mathbf{S}_2 \cdot \mathbf{S}_3 \quad (\text{A.2})$$

where one notes the absence of first-neighbor, second-neighbor, and sixth-neighbor interactions.

One may perform DFT-GGA calculations, and obtain the total energies for SQS configurations with all Mn

$S = 5/2$ atoms aligned with each other, as well as for an increasing number of flipped Mn total spins. The total-energy differences with respect to the aligned states, $\{\Delta E\}$, may then be obtained via an effective classical Heisenberg model with appropriate J_n exchange couplings up to $n = 6$.

For the disorder configuration in Fig. 1(a), noticing that classically one has $\mathbf{S}_i \cdot \mathbf{S}_j = \pm \frac{25}{4}$, it is straightforward to obtain, using eq. (A.1), for the total energies of configurations with appropriate flipping of Mn total spins

$$E_0 = \frac{25}{4}(+J_1 + J_3 + 4J_6) \quad (\text{A.3})$$

$$E_1^1 = \frac{25}{4}(-J_1 + J_3 - 4J_6) \quad (\text{A.4})$$

$$E_1^2 = \frac{25}{4}(-J_1 - J_3 + 4J_6) \quad (\text{A.5})$$

$$E_1^3 = \frac{25}{4}(+J_1 - J_3 - 4J_6), \quad (\text{A.6})$$

where the lower index indicates the number of flipped spins (from $+5/2$ to $-5/2$), and the upper index labels which spin was flipped. The differences in corresponding Heisenberg energies are therefore

$$\Delta_{1-0} = -\frac{25}{4}(2J_1 + 8J_6) \quad (\text{A.7})$$

$$\Delta_{2-0} = -\frac{25}{4}(2J_1 + 2J_3) \quad (\text{A.8})$$

$$\Delta_{3-0} = -\frac{25}{4}(2J_3 + 8J_6), \quad (\text{A.9})$$

and one may thus obtain $J_1 = -16.2$ meV, $J_3 = -3.0$ meV, and $J_6 = -1.2$ meV from the calculated first principles differences in total energies, i.e., $\Delta_{1-0} = 264$ meV, $\Delta_{2-0} = 241$ meV, and $\Delta_{3-0} = 99$ meV.

-
- ¹ *Semiconductor and Semimetals*, vol. 25 (Academic, New York, 1988), edited by J. K. Furdyna and J. Kossut.
 - ² H. Ohno, H. Munekata, T. Penney, S. von Molnàr, and L. L. Chang, *Phys. Rev. Lett.* **68**, 2664 (1992).
 - ³ H. Ohno, A. Shen, F. Matsukura, A. Oiwa, A. Endo, S. Katsumoto, and Y. Iye, *Appl. Phys. Lett.* **69**, 363 (1996).
 - ⁴ A. V. Esch, L. V. Bockstal, J. D. Boeck, G. Verbanck, A. S. van Steenbergen, P. J. Wellmann, B. Grietens, R. Bogaerts, F. Herlach, and G. Borghs, *Phys. Rev. B* **56**, 13103 (1997).
 - ⁵ F. Matsukura, H. Ohno, A. Shen, and Y. Sugawara, *Phys. Rev. B* **57**, R2037 (1998).
 - ⁶ H. Ohno, *J. Magn. Magn. Mater.* **200**, 110 (1999).
 - ⁷ S. J. Potashnik, K. C. Ku, S. H. Chun, J. J. Berry, N. Samarth, and P. Schiffer, *Appl. Phys. Lett.* **79**, 1495 (2001).
 - ⁸ K. W. Edmonds, K. Y. Wang, R. P. Campion, A. C. Neumann, C. T. Foxon, B. L. Gallagher, and P. C. Main, *Appl. Phys. Lett.* **81**, 3010 (2002).
 - ⁹ M. J. Seong, S. H. Chun, H. M. Cheong, N. Samarth, and A. Mascarenhas, *Phys. Rev. B* **66**, 033202 (2002).
 - ¹⁰ H. Asklund, L. Ilver, J. Kanski, and J. Sadowski, *Phys. Rev. B* **66**, 115319 (2002).
 - ¹¹ K. M. Yu, W. Walukiewicz, T. Wojtowicz, I. Kuryliszyn, X. Liu, Y. Sasaki, and J. K. Furdyna, *Phys. Rev. B* **65**, 201303 (2002).
 - ¹² K. M. Yu, W. Walukiewicz, T. Wojtowicz, W. L. Lim, X. Liu, Y. Sasaki, M. Dobrowolska, and J. K. Furdyna, *Appl. Phys. Lett.* **81**, 844 (2002).
 - ¹³ S. J. Potashnik, K. C. Ku, R. Nahendiran, S. H. Chun, R. F. Wang, N. Samarth, and P. Schiffer, *Phys. Rev. B* **66**, 012408 (2002).
 - ¹⁴ R. Moriya and H. Munekata, *J. Appl. Phys.* **93**, 4603 (2002).
 - ¹⁵ R. R. dos Santos, L. E. Oliveira, and J. d'Albuquerque e Castro, *J. Phys.: Cond. Matter* **14**, 3751 (2002).
 - ¹⁶ R. R. dos Santos, J. d'Albuquerque e Castro, and L. E. Oliveira, *J. Appl. Phys.* **93**, 1845 (2003).
 - ¹⁷ M. van Schilfgaarde and O. N. Mryasov, *Phys. Rev. B* **63**, 233205 (2001).
 - ¹⁸ J. L. Xu, M. van Schilfgaarde, and G. D. Samolyuk, *Phys. Rev. Lett.* **94**, 097201 (2005).
 - ¹⁹ J. Kudrnovský, I. Turek, V. Drchal, F. Máca, P. Weinberger, and P. Bruno, *Phys. Rev. B* **69**, 115208 (2004).
 - ²⁰ J. Kudrnovský, V. Drchal, I. Turek, L. Berqvist, O. Eriksson, G. Bouzerar, L. Sandratskii, and P. Bruno, *J. Phys.: Cond. Matter* **16**, S5571 (2004).
 - ²¹ L. Bergqvist, O. Eriksson, J. Kudrnovský, V. Drchal, P. Korzhavyi, and I. Turek, *Phys. Rev. Lett.* **93**, 137202 (2004).

- (2004).
- ²² K. Sato, H. Katayama-Yoshida, and P. H. Dederichs, J. Superconductivity **16**, 31 (2003).
 - ²³ K. Sato, W. Schweika, P. H. Dederichs, and H. Katayama-Yoshida, Phys. Rev. B **70**, 201202 (2004).
 - ²⁴ L. M. Sandratskii and P. Bruno, Phys. Rev. B **66**, 134435 (2002).
 - ²⁵ L. M. Sandratskii and P. Bruno, Phys. Rev. B **67**, 214402 (2003).
 - ²⁶ L. M. Sandratskii and P. Bruno, J. Phys.: Cond. Matter **16**, L523 (2004).
 - ²⁷ D. Vanderbilt, Phys. Rev. B **41**, 7892 (1990).
 - ²⁸ G. Kresse and J. Hafner, Phys. Rev. B **47**, R558 (1993).
 - ²⁹ P. Mahadevan and A. Zunger, Phys. Rev. B **69**, 115211 (2004).
 - ³⁰ S. H. Wei, L. G. Ferreira, J. E. Bernard, and A. Zunger, Phys. Rev. B **42**, 9622 (1990).
 - ³¹ A. J. R. da Silva, A. Fazzio, R. R. dos Santos, and L. E. Oliveira, Physica B **340-342**, 874 (2003).
 - ³² A. J. R. da Silva, A. Fazzio, R. R. dos Santos, and L. E. Oliveira, J. Phys.: Cond. Matter **16**, 8243 (2004).
 - ³³ G. Kresse and D. Joubert, Phys. Rev. B **59**, 1758 (1999).
 - ³⁴ J. Schliemann and A. H. MacDonald, Phys. Rev. Lett. **88**, 137201 (2002).
 - ³⁵ G. Zaránd and B. Jankó, Phys. Rev. Lett. **89**, 047201 (2002).
 - ³⁶ P. Mahadevan, A. Zunger, and D. D. Sarma, Phys. Rev. Lett. **93**, 177201 (2004).
 - ³⁷ P. Mahadevan, J. M. Osorio-Guillén, and A. Zunger, Appl. Phys. Lett. **86**, 172504 (2005).
 - ³⁸ A. H. MacDonald, P. Schiffer, and N. Samarth, Nature Mat. **4**, 195 (2005).
 - ³⁹ V. F. Sapega, M. Moreno, M. Ramsteiner, L. Däweritz, and K. H. Ploog, Phys. Rev. Lett. **94**, 137401 (2005).
 - ⁴⁰ D. Stauffer and A. Aharony, *Introduction to Percolation Theory* (Taylor & Francis, London, 1992), 2nd Ed.
 - ⁴¹ D. J. Priour, Jr., E. H. Hwang, and S. Das Sarma, Phys. Rev. Lett. **92**, 117201 (2004).
 - ⁴² C. Timm and A. H. MacDonald, Phys. Rev. B **71**, 155206 (2005).
 - ⁴³ A. J. R. da Silva and L. M. Falicov, Phys. Rev. B **52**, 2325 (1995).